Bacterial Fe(II)-oxidation Distinguished by Long-Range Correlation in Redox Potential

Allison M.L. Enright and F. Grant Ferris
University of Toronto
Department of Earth Sciences
22 Russell St
Toronto, ON
M5S 3B1

This article has been accepted for publication and undergone full peer review but has not been through the copyediting, typesetting, pagination and proofreading process which may lead to differences between this version and the Version of Record. Please cite this article as doi: 10.1002/2015JG003306

Abstract

The kinetics of bacterial Fe(II)-oxidation was investigated 297 m underground at the Äspö Hard Rock Laboratory (near Oskarshamn, Sweden) under steady state groundwater flow conditions in a flow-through cell containing well developed flocculent mats of bacteriogenic iron oxides (BIOS). Pseudo-first order rate constants of 0.004 min^{-1} and 0.009 min^{-1} were obtained for chemical and bacterial Fe(II)-oxidation, respectively, based on the 104 minute retention time of groundwater in the flow cell, inlet Fe(II) concentration of 21.0 ± 0.5 μM, outlet Fe(II) concentration of 8.5 ± 0.7 μM, as well constant pH of 7.42 ± 0.01, dissolved O_2 concentration of 0.11 ± 0.01 mg/L, and groundwater temperature of 12.4 ± 0.1 ^{o}C. Redox potential was lower at the BIOS-free inlet (-135.4 ± 1.16 mV) compared to inside BIOS within the flow cell (-112.6 ± 1.91 mV), consistent with the Nernst relationship and oxidation of Fe(II) to Fe(III). Further evaluation of the redox potential time series data using detrended fluctuation analysis (DFA) revealed power-law scaling in the amplitude of fluctuations over increasing intervals of time with significantly different ($p < 0.01$) DFA α scaling exponents of 1.89 ± 0.03 for BIOS and 1.67 ± 0.06 at the inlet. These α values not only signal the presence of long-range correlation in the redox potential time series measurements, but also distinguish between the slower rate of chemical Fe(II)-oxidation at the inlet and faster rate accelerated by FeOB in BIOS.

Key Points

- Electrochemical methods permit in situ characterization of microbial environments.
- Fluctuations in redox potential arise from elementary electrochemical reactions.
- Long-range correlations of redox potential indicate the presence of anomalous diffusion.

Index Terms

0412 Biogeochemical kinetics and reaction modelling

0448 Geomicrobiology

Key Words

- Iron-oxidizing bacteria;
- Oxidation-reduction potential;
- Fluctuation analysis.

1. Introduction

Chemolithotrophic bacteria derive energy from the oxidation of reduced inorganic substances [*Tolli and King, 2005; Bailey et al., 2009; Bethke et al., 2011; Boyd et al., 2014; Converse et al., 2015*]. Bacterial oxidation of Fe(II) is particularly significant because of its role as one of the earliest forms of metabolism on Earth, and its contributions to global biogeochemical cycling and physicochemical speciation of iron [*Ferris, 2005; Weber et al., 2006; Bird et al., 2011; Emerson 2012; Melton et al., 2014*]. At circumneutral pH, rapid chemical oxidation of Fe(II) in the presence of atmospheric oxygen restricts Fe(II)- oxidizing bacteria (FeOB) to low pO_2 environments where chemical oxidation is slower [*Anderson and Pedersen, 2003; James and Ferris, 2004; Anderson et al., 2006; Druschel et al., 2008; Vollrath et al., 2012; Vollrath et al., 2013*]. In environments where neutrophilic Fe(II)-oxidizing bacteria compete with chemical oxidation, rapid hydrolysis and precipitation of Fe(III) produces flocculent mats of bacteriogenic iron oxides (BIOS) consisting of poorly-ordered hydrous ferric-oxides (HFO) intermixed with bacterial cells [*Kennedy et al., 2003; Kennedy et al., 2004; Toner et al., 2009; Chan et al., 2011; Suzuki et al., 2011; Gault et al., 2012; Ferris et al., 2015*].

Although knowledge of the widespread environmental occurrence and diversity of circumentural FeOB continues to grow [*Weber et al., 2006; Emerson 2012; Fleming et al., 2014*], understanding the complex heterogeneous dynamics of interconnected chemical and bacterial Fe(II)-oxidation remains as a major challenge in biogeochemistry [*Vollrath et al., 2012; Vollrath et al., 2013; Melton et al., 2014; Barco et al., 2015*]. Inhibition of respiratory metabolism using azide as a poison has been used widely to distinguish chemical from bacterial Fe(II) oxidation in laboratory and microcosm experiments [*James and Ferris, 2004; Rentz et al., 2007; Druschel et*

al., 2008]; however, use of a metabolic poison for *in situ* environmental investigations is decidedly contraindicated. An alternative approach is the application of electrochemical based measurements that not only alleviate the need to recover and manipulate samples in experiments with toxic chemicals, but also allow for high rates of data acquisition in relatively short periods of time [*Taillefert et al., 2000*]. Determination of redox potential, in particular, is regarded almost universally as a good indicator for the prediction of microbial mediated oxidation-reduction transformations and energy flow in natural systems [*Stumm and Morgan, 1996*].

Continuous measurements of redox potential in field studies and laboratory experiments are usually interpreted in terms of broad shifts, typically on the order of > 100 mV over a period of days to months that are taken as an indication of changes between oxidizing and reducing conditions with a concomitant succession of microbial communities [*Seybold et al., 2002; Van Bochove et al., 2002; Nikolausz et al., 2008; Parsons et al., 2013*]. On shorter time scales, fluctuations in redox potential tend to be taken as random noise despite falling within the minute to second range of reaction half-times of chemolithotrophic electron transfer metabolisms, as exemplified by bacterial Fe(II)-oxidation [*James and Ferris 2004; Rentz et al., 2007; Druschel et al., 2008; Vollrath et al., 2012; Vollrath et al., 2013*]. At the same time, considerable evidence exists to show that fluctuating signals in complex heterogeneous dynamical systems contain useful information pertaining to underlying determinative physicochemical processes [*Hassibi et al., 2004; Delignieres et al., 2006; Hardstone et al., 2012; Eliazar and Shlesinger, 2013*]. The emergence of long-range correlation, also known as persistence or memory, is of particular interest as it stems from power-law decay of statistical dependence between adjacent and distantly neighboured measurements of physical quantities

characterizing the dynamics of complex systems with numerous interacting components [*Metzler and Klafter, 2000; Grigolini et al., 2001*]. In essence, long-range correlation in a time series means that any given value is statistically dependent on preceding values; positive correlation signifies that an increasing trend in the past is likely to be followed by an increasing trend in the future, whereas negative correlation signifies that a increasing trend in the past is likely to be followed by a decreasing trend in the future [*Delignieres et al., 2006; Witt and Malamud, 2013*]

This paper addresses the detection and quantification of long-range correlations embedded in time series measurements of redox potential acquired under steady state groundwater flow conditions in a flow-through cell containing well developed flocculent mats of FeOB and BIOS. The strength of long-range correlations were inferred from power law scaling exponents of fluctuations in redox potential as determined using the widely applied computational method of detrended fluctuation analysis (DFA) [*Peng et al., 1994; Scafetta and Grigolini, 2002; Delignieres et al., 2006; Bryce and Sprague, 2012; Hardstone et al., 2012; Shao et al., 2012; Witt and Malamud, 2013*]. Rates of Fe(II)-oxidation were established based on the retention time of groundwater in the flow cell along with the difference between inlet and outlet concentrations of Fe(II) [*Coker, 2001*].

Strong long-range correlations in redox potential fluctuations are reported for high rates of bacterial Fe(II)-oxidation, while being weaker for slower rates in the absence of bacteria. As an explanation for these results, it is hypothesized that coupled diffusion-reaction processes in Fe(II)-oxidation give rise to anomalous diffusive transport, which manifests as long-range correlations of redox potential fluctuations [*Gabrielli et al., 1993; Hassibi et al., 2004; Metzler and Klafter, 2000;*

Grigolini et al, 2001; Stewart, 2003; Petroff et al., 2011; Eliazar and Shlesinger, 2013; Hofling and Franosch, 2013; Jeon et al., 2014]. Depending on the strength of such long-range correlations, distinction between slower abiotic Fe(II)-oxidation rates and faster rates associated with FeOB is entirely feasible.

2. Methods

2.1 Site Description

The study was conducted 297 m underground at experimental site 2200A in the Äspö Hard Rock Laboratory (HRL) near Oskarshamn on the Baltic coast of Sweden (599685 m E 6366835 m N UTM zone 33V). At the site, groundwater from a hydraulically conductive fracture is delivered at a flow rate of 0.65 L min^{-1} from a packed-off section of borehole KA2198A through round 0.6 cm stainless steel tubing to a 200 x 30 x 25 cm (length x width x height) flow cell; photographs and a diagram of the flow cell are provided in earlier reports [*Anderson and Pedersen, 2003; Anderson et al., 2006*]. Groundwater enters into a 20 cm-long inlet compartment that is separated from the main length of the cell by a perforated baffle. The main chamber of the flow cell is approximately half-filled with granite cobble [*Anderson and Pedersen, 2003*], giving a nominal volume of 68 L and groundwater residence time of 104 minutes. To ensure steady state biogeochemical conditions before experimentation, the flow through cell was allowed to operate undisturbed, open to air, in the dark for a period of 12 months, allowing a natural community of *Gallionella ferruginea* and other FeOB to develop and form extensive accumulations of flocculent orange-colored BIOS [*Anderson et al., 2006*]. The inlet chamber remained devoid of BIOS over the entire interval of time. Details concerning the hydrogeology of the borehole and development of BIOS have been described previously [*Anderson and Pedersen, 2003],* as has the microbiology of these fluids [*Anderson et al., 2006*].

2.2 Data Acquisition

Continuous monitoring of pH, temperature, dissolved O_2 and redox potential was accomplished using a YSI Environmental QS 600 multiple electrode sonde and YSI EcoWatch® data logging software. After mounting on a retort stand, the sonde was submerged to position all electrodes and sensors at a depth of approximately 12.5 cm at the groundwater inlet and midway along the length flow cell in the BIOS. Measurements were recorded at one second intervals (i.e., at a data acquisition frequency of 1 Hz) for approximately 40 minutes with pH and redox potential readings measured relative to a standard Ag^0/AgCl reference electrode.

2.3 Geochemical Analysis

Water samples were collected three times over 24 hours from the inlet and outlet of the flow cell; 2 hours before the start of continuous pH, temperature, dissolved O_2 and redox potential monitoring, then 2 hours and 20 hours afterwards. The samples were collected by completely filling sterile 500 mL acid-washed polypropylene bottles, taking care to leave no head-space for air,and 250 mL aliquots were vacuum filtered using 0.22 µm-pore-size membrane filters in accordance with standard protocols for determination of dissolved Fe(II) and Fe(III) [*Rentz et al., 2007; Druschel et al., 2008; Vollrath et al., 2012; Vollrath et al., 2013*]. Concentrations of total Fe and Fe(II) were measured in triplicate on site immediately after filtration using a HACH DR/2500 spectrophotometer with FerroVer® and 1,10 phenanthroline reagents (HACH), respectively, with a 0.18 µM limit of detection. The concentrations of Fe(III) were calculated afterwards as the difference between measured total Fe and Fe(II) concentrations.

2.4 Detrended Fluctuation Analysis

Integrated random walk profiles of the redox potential time series data were compiled for DFA by computing the cumulative difference of each measurement from the mean of the entire series [*Peng et al., 1994; Delignieres et al., 2006; Bryce and Sprague, 2012; Shao et al., 2012*]. The profiles were then divided into non-overlapping time intervals of equal length s and detrended by subtracting linear least square fits of data in each interval. Characteristic fluctuation amplitudes of local linear trend residual differences were calculated afterwards as root mean square (RMS) deviations averaged across the corresponding number of time intervals. This computation was repeated using eight different time intervals ranging from 20 s to 1250 s in length. For long-range correlations in time series, RMS fluctuation amplitudes typically increase with s following a power law relationship

$$RMS \propto s^{\alpha} \qquad (1)$$

where scaling exponent α is determined as the slope of a double logarithmic plot of RMS values as a function of time interval length s [*Peng et al., 1994; Delignieres et al., 2006; Bryce and Sprague, 2012*]. In random uncorrelated time series α = 0.5, whereas $|\alpha - 0.5| < 0$ is indicative of long-range correlation.

For this investigation, DFA was implemented in MatLAB. Input data included the observed inlet and BIOS 1.0 Hz redox potential time series measurements (*n* = 2500), as well as a pool of shorter realizations (i.e., two *n* = (2500/2) = 1250 and four *n* = 1000 starting at initial times of 0, 501, 1001, and 1501 seconds, respectively). As a procedural control for the detection of long-range correlations, DFA was also performed after randomly shuffling each input time series using the 'rand' function in MatLAB.

3. Results

3.1 Physicochemical Conditions

Measurements for inlet temperature, pH, redox potential and dissolved O_2 indicated stable conditions throughout the period of continuous measurement in the flow cell (Figure 1); vertical variations are assumed to be minimal as determined previously [*Anderson et al., 2006*]. Specifically, temperature and pH remained steady near 12.4 ± 0.1 ^{o}C and 7.42 ± 0.01, respectively, with dissolved O_2 around 0.11 ± 0.01 mg/L. Observed temperature, pH, and dissolved O_2 were the same at the mid-point of the flow cell in the BIOS; however, mean redox potential was lower at the inlet (i.e., mean value of -135.4 ± 1.16 mV) than in the BIOS (i.e., mean value of -112.6 ± 1.91 mV). The inlet and outlet concentrations of dissolved Fe(II) remained constant within standard errors of measurement over the 24 hour period before and after the interval of continuous monitoring of pH, temperature, dissolved O_2 and redox potential (Table 1). Total Fe and Fe(II) concentrations were greater at the inlet than the outlet concentrations, whereas Fe(III) concentrations (calculated as the difference between total Fe and Fe(II) concentrations) were the same at both the inlet and the outlet. These quantities are an expression of a dynamic steady state where the overall system chemistry is balanced by a combination of material fluxes and chemical reactions. Specifically, the oxidation of Fe(II) accounts for the observed decrease in concentration from 21.0 ± 0.5 μM at the inlet to 8.5 ± 0.7 μM at the outlet. Similarly, mass balance constraints associated with the hydrolysis and precipitation of Fe(III) as HFO accounts for the lower total Fe concentration at the outlet. Moreover, similar concentrations of dissolved Fe(III) at the inlet and outlet suggest that rates of Fe(II)-oxidation and HFO precipitation balance each other.

3.2 Fe(II)- oxidation Rates

The rate law for the oxidation of Fe(II) by O_2 can be written as

$$-\frac{\mathrm{d[Fe(II)]}}{\mathrm{dt}} = \frac{k_{ox}[\mathrm{O_2}]}{[\mathrm{H^+}]^2}[\mathrm{Fe(II)}] \qquad (2)$$

with the overall fourth-order rate constant k_{ox} = 9.9 x 10^{-7} μmol L^{-1} min^{-1} for the measured inlet temperature of 12.4 ^{o}C [*Stumm and Morgan, 1996*]. At constant pH and dissolved O_2 concentration, the rate expression becomes pseudo-first order with respect to Fe(II)

$$-\frac{\mathrm{d[Fe(II)]}}{\mathrm{dt}} = k'_{ox}[\mathrm{Fe(II)}] \qquad (3)$$

with the pseudo-first order rate constant, k'_{ox}

$$k'_{ox} = \frac{k_{ox}[\mathrm{O_2}]}{[\mathrm{H^+}]^2} \qquad (4).$$

Assuming steady-state conditions within the flow cell, with a uniform flow field and negligible hydrodynamic dispersion along the principal axis of the flow cell, the fraction of un-oxidized Fe(II) remaining at the outlet is given by [*Coker, 2001*]

$$\frac{[\mathrm{Fe(II)}]_{\mathrm{Outlet}}}{[\mathrm{Fe(II)}]_{\mathrm{Inlet}}} = \exp - k'_{ox}\tau \qquad (5)$$

Considering that the groundwater residence time τ = 104 minutes, an inlet concentration $[\mathrm{Fe(II)}]_{\mathrm{Inlet}}$ = 21.0 μM, and outlet concentration $[\mathrm{Fe(II)}]_{\mathrm{Outlet}}$ = 8.5 μM, then the pseudo-first order rate constant for Fe(II) oxidation k'_{ox} = 0.009 min^{-1}. At the measured pH and dissolved oxygen concentration in the flow cell, this is more than double the expected value from equation 3 of 0.004 min^{-1} for chemical oxidation. The observation of accelerated Fe(II) oxidation kinetics in the flow cell is consistent with other studies on bacterial oxidation of Fe(II), which indicate that biological activity can result in as much as a 10-fold increase in oxidation rates, depending on

bacterial biomass concentrations [*James and Ferris, 2004; Rentz et al., 2007; Druschel et al., 2008*].

For an accelerated overall rate that combines chemical and bacterial Fe(II) oxidation, the fractional contribution of bacteria f corresponds to

$$f = \frac{k_{bac}[B]}{k'_{ox}} \qquad (6)$$

where $k_{bac} = 0.067$ L g-1 min^{-1} is a pseudo-second order rate constant for the dependency Fe(II) oxidation on bacterial dry weight concentration B in BIOS [*Ferris et al., in press*]. Previous measurements of steady ATP biomass in the flow cell give contrasting bacterial dry weight concentrations of 0.028 mg mL^{-1} (2.76 x 10^4 cells mL^{-1}) at the inlet, and 273 mg mL^{-1} (2.73 x 10^8 cells mL^{-1}) for the BIOS [*Anderson et al., 2006*]. At the bacterial concentration at the inlet, f is almost negligible at 0.0002 in comparison to 0.55 in the BIOS. In terms of rates, at the inlet, with an Fe(II) concentration of 21 μM and $k'_{ox} = 0.004$ min^{-1}, the rate of chemical oxidation would be 0.084 μmol L^{-1} min^{-1}. Midway through the flow cell use of equation 5, with a halved residence time of 52 minutes and BIOS $k'_{ox} = 0.009$ min^{-1}, predicts a decreased Fe(II) concentration of 13.2 μM, which equates to an apparent chemical oxidation rate of 0.053 μmol L^{-1} min^{-1} and bacterial accelerated oxidation rate of 0.118 μmol L^{-1} min^{-1}. Ascribing the difference of 0.065 μmol L^{-1} min-1 between chemical and bacterial accelerated rates of Fe(II) oxidation gives an apparent fractional contribution of 0.55, as predicted from biomass concentrations by equation 6.

3.3 Detrended Fluctuation Analysis

Inlet and BIOS redox potential measurements for 120 s time intervals are shown in Figure 2, as are shuffled redox potential time series and corresponding

random walk profiles. At the 1 Hz measurement frequency, incremental steps in inlet and BIOS redox potential display more of a regular cyclical pattern than the shuffled data. Similarly, the inlet and BIOS mV random walk profiles are smoother and traverse persistently over greater lengths of time compared to the random walk profiles of the shuffled data.

A double logarithmic plot of RMS fluctuation amplitudes in observed and shuffled random walk redox potential profiles as a function of time interval is shown in Figure 3. These plots reveal typical power law scaling behavior and show how RMS deviations of redox potential fluctuations increase nonlinearly over longer intervals of time. The corresponding scaling exponent for redox potential fluctuations in the BIOS was 1.89 ± 0.03 compared to 1.67 ± 0.06 for the inlet (Table 2). In one-sided *t*-tests, the inlet and BIOS α values were significantly different at a level of $p < 0.01$. These α values signal the existence of strong long-range correlation in redox potential fluctuations both in the presence and absence of BIOS, whereas α scaling exponents of 0.50 and 0.51 in the shuffled data describe random uncorrelated time series; however, the higher BIOS α value was recovered for an accelerated bacterial Fe(II) oxidation rate of 0.118 μmol L^{-1} min^{-1} compared to only 0.084 μmol L^{-1} min^{-1} for the lower α scaling exponent at the inlet. The implication is that the higher α value for the BIOS distinguishes bacterial from predominantly chemical oxidation under otherwise identical geochemical conditions.

4. Discussion

4.1 Fe(II) Oxidation Kinetics

The measured steady state geochemical conditions in the flow cell match previously reported stable values for temperature, pH, dissolved oxygen, and redox potential [*Anderson and Pederson, 2003*]. Similarly, the observed decrease in total

dissolved Fe owing to the oxidation of Fe(II) and subsequent precipitation of oxidized Fe(III) agrees with earlier results [*Anderson et al., 2006*]. In terms of electrochemical behavior, the higher redox potential in the BIOS compared to the inlet is explained by an increase in Fe(III)/Fe(II) ratio associated with the metabolic activity of FeOB. This is expected from the Nernst relationship, which predicts that redox potential should increase with an increasing proportion of oxidized species in solution; in fact, redox potential values calculated for the Fe(II)/Fe(III) redox couple of -137.7 mV for the inlet and -115.0 mV for the BIOS compare favorably with measured inlet and BIOS redox potentials of -135.4 mV and -112.6 mV, respectively [*Stumm and Morgan, 1996*].

Investigations on relative chemical and bacterial contributions to Fe(II) oxidation kinetics at circumneutral pH and low dissolved oxygen concentrations emphasize the additional coincident importance of cell density and temperature [*Druschel et al., 2008; Vollrath et al., 2013; Ferris et al., 2015*]. A recent study with the Fe(II)-oxidizer *Leptothrix chlolodnii*, conducted at the same cell density (i.e., ~ 10^8 cells mL^{-1}) that was observed in the flow cell, found pseudo-first order rate constants increasing from 0.004 min^{-1} at 11.4 ^oC to 0.249 min^{-1} at 37.9 ^oC, which corresponds to an activation energy of 114 kJ mol^{-1} [*Vollrath et al., 2013*]. In a separate study with *Siderooxydans lithotrophicus*, carried out at a cell density of 2 x 10^7 cells mL^{-1} and 21.5 ^oC, estimates for pseudo-first order rate constants ranged from 0.030 min^{-1} to 0.065 min^{-1} [*Druschel et al., 2008*]; the range is lower at 0.007 to 0.015 min^{-1} when corrected to the measured flow cell water temperature of 12.4 ^oC using the Arrhenius equation [*Stumm and Morgan, 1996*]. This puts the BIOS rate constant value of 0.009 min^{-1} determined for the flow cell well within the range of values reported for bacterial Fe(II) oxidation at low groundwater temperatures and

cell densities in the order of 10^7 to 10^8 cells mL^{-1}. In the absence of bacteria, Fe(II)-oxidation kinetics are slower with experimental estimates of pseudo-first order rate constants generally between 0.001 min^{-1} and 0.007 min^{-1} at 12.4 ^oC, corresponding to the estimate of 0.004 min^{-1} for the flow cell [*Druschel et al., 2008; Vollrath et al., 2013*].

The prevailing consensus is that oxidization of Fe(II) by bacteria at circumneutral pH takes place outside the cell, leaving produced Fe(III) subject to hydrolysis and eventual precipitation as HFO [*Bird et al., 2011; Suzuki et al., 2011; Emerson, 2012; Melton et al., 2014; Barco et al., 2015*]. Diffusion mediates cellular interception of reduced Fe(II), as well as the escape of oxidized Fe(III) species, with rates of oxidation, hydrolysis, and precipitation implicitly shaping the coinciding concentration gradients [*Stewart 2003; Petroff et al., 2011*]. These aspects of reactive mass transport in bacterial Fe(II) oxidation are noteworthy as redox potential measurements are subject to fluctuations caused by coupled diffusion-reaction processes [*Gabrielli et al., 1993; Hassibi et al., 2004*]. Consequently, it is quite reasonable to surmise that the observed fluctuations of inlet and BIOS redox potential stem from a combination of elementary electrochemical reactions involving electron transfer and mass transport of dissolved chemical species involved in the oxidation-reduction process.

4.2 Long-range Correlation in Redox Potential Fluctuations

The detection and quantification of long-range correlations in inlet and BIOS redox potential fluctuations using DFA emphasizes the underlying complexity and heterogeneous nature of bacterial Fe(II) oxidation [*James and Ferris, 2004; Rentz et al., 2007; Vollrath et al., 2012; Melton et al., 2014*]. This is one of the recognized strengths of DFA, namely that $|\alpha - 0.5| > 0$ reveals departures from idealized

system dynamics in complex systems [*Shao et al., 2012*]. Moreover, determination of different DFA scaling exponents of 1.67 and 1.89 for the inlet and BIOS redox potential fluctuations, respectively, provides a compelling electrochemical-based statistical distinction between slower, predominantly chemical, oxidation of Fe(II) at the inlet and Fe(II) oxidation accelerated by bacteria in BIOS. In contrast, existing evidence distinguishing chemical and bacterial Fe(II) oxidation comes almost exclusively from experimental studies that compared changes in Fe(II) concentrations over time in pure cultures of FeOB or mixed microbial BIOS microcosms to corresponding cell-free and poisoned controls [*James and Ferris, 2004; Rentz et al., 2007; Druschel et al., 2008; Vollrath et al., 2012; Vollrath et al., 2013; MacDonald et al., 2014*].

At the molecular level, the existence of long-range correlations in redox potential fluctuations can be interpreted in terms of cumulative translocations of reduced and oxidized species undergoing reaction and diffusion [*Hassibi et al., 2004; Haugh, 2009*]. The expected DFA result for random uncorrelated Brownian motion in normal, (i.e., Fickian) diffusion processes is a scaling exponent of 0.5 [*Grigolini et al., 2001*], as observed with shuffled redox potential time course data for the inlet and BIOS. Conversely, long-range correlations determined for measured inlet and BIOS redox potential time series are reflective of fractional Brownian motion and anomalous (i.e., non-Fickian) diffusion where the squared displacement of diffusing species over time (t) is proportional to $t^{2\eta}$ [*Metzler and Klafter, 2000; Haugh, 2009*]; the DFA α value is a generalization of scaling exponent η such that $\eta = \alpha$ for fractional Gaussian processes in which $\alpha \in$ [0,1] and $\eta = \alpha - 1$ for fractional Brownian motion with $\alpha \in$ [1,2] [*Delignieres et al., 2006*]. The strong long-range correlation evident in the BIOS redox potential fluctuations, in particular, fits the

definition of anomalous diffusion with a faster overall rate of Fe(II) oxidation arising from the metabolic involvement of bacteria and expectation of strong localized concentration gradients around active cells [*Stewart, 2003; Petroff et al., 2011*]. In contrast, the weaker correlation in redox potential fluctuations at the inlet is manifest for a slower rate of chemical Fe(II) oxidation with essentially no involvement of bacteria, implying a lower degree of anomalous diffusion behavior than observed for FeOB in BIOS.

4.3 Biogeochemical Significance

Determination of nonlinear redox potential scaling exponents for Fe(II)-oxidation using DFA and the evident relation to anomalous diffusion behavior is significant on two accounts. First, an increased level of correlation (i.e., higher α value) signals an elevated reaction rate that can be attributed to bacterial activity and metabolic electron transport-mediated oxidation coupled to diffusional transport. This not only emphasizes the fundamental importance of interactively linked reaction-diffusion processes in bacterial Fe(II)-oxidation [*Stewart 2003; Petroff et al., 2011*], but also that FeOB can outcompete the kinetics of abiotic homogeneous oxidation of Fe(II) in solution, as well as autocatalytic heterogeneous Fe(II) oxidation on HFO precipitates [*James and Ferris, 2004; Rentz et al., 2007; Druschel et al., 2008; Vollrath et al., 2012; Vollrath et al., 2013*]. Second, the ability to distinguish between chemical and bacterial oxidation of Fe(II) by electrochemical means raises the intriguing possibility of using DFA α scaling exponents of redox potential fluctuations as an intensity parameter for microbial activities associated with other types of electron-transfer metabolisms involving C, H, O, N, S, and trace metals [*Bethke et al., 2011*]. Insight concerning how active bacteria are in nature is especially important for understanding their fundamental impact on biogeochemical

cycles, as well as their effectiveness in bioremediation and biotechnology *[Bird et al., 2011; Melton et al., 2014*]. Another aspect to consider is that environmental sampling for conventional chemical and biological analyses is not trivial because samples are frequently difficult to access (e.g., remote locations, sediment porewaters, groundwaters), and physicochemical changes (e.g., exposure to atmospheric oxygen, alteration of temperature) may occur during sampling. The application of *in situ* electrochemical measurements is regarded as a good alternative to circumvent such problems [*Taillefert et al., 2000; van Bochove et al., 2002*], and this lends strong practical support to the idea of using redox potential measurements and DFA α scaling exponents to evaluate microbial contributions to biogeochemical processes.

5. Conclusion

The results of this investigation demonstrate that scaling exponents obtained from DFA of redox potential time series measurements offer valuable insight into the dynamics and biogeochemical behavior of microbial Fe(II)-oxidizing systems. A major advantage of this approach is that it does not require chemical analyses of metabolites, relying instead on electrochemical measurement of oxidation-reduction potential. The significance of this result could be profound since DFA scaling exponents for fluctuations in redox potential permit distinction between predominantly chemical versus bacterially accelerated oxidation-reduction processes. While biological activity was not strictly excluded here, the use of DFA to derive a scaling exponent for fluctuations in redox potential that can be attributed to the activity of FeOB holds promise as an electrochemical based method for *in situ* studies of bacterial electron-transfer metabolisms. It might even be possible to use scaling exponents from redox potential time series measurements in an

astrobiological context as a biogeophysical signature for life. An additional prospect to consider is the use of ion-specific electrodes to assess bacterial transformations among specific redox active chemical species of interest, instead of relying exclusively on the general parameter of redox potential. Overall, the results are promising and suggest that the sensitivity of redox potential to bacterial activity, and the field of fluctuation analysis in general, have promise for biogeophysical studies in environmental microbiology.

Acknowledgements

This work was supported by NSERC Discovery Grant to F.G. Ferris. Data files for DFA analysis available at <<https://www.researchgate.net/profile/F_Ferris>>.

References

Anderson, C. R., and K. Pedersen (2003), In situ growth of Gallionella biofilms and partitioning of lanthanides and actinides between biological material and ferric oxyhydrides, *Geobiology*, 1, 169-178.

Anderson, C.R., R.E. James, E.C. Fru, E.B. Kennedy, and K. Pedersen (2006), In situ ecological development of a bacteriogenic iron oxide-producing microbial community from a subsurface granitic rock environment, *Geobiology*, 4, 29-42.

Barco, R.A., D. Emerson, J.B. Sylvan, B.N. Orcutt, M.E. Jacobson Myers, G.A. Ramfrez, J.D. Zhong, and K.J. Edwards (2015), New insight into microbial iron oxidation as revealed by the proteomic profile of an obligate iron-oxidizing chemolithoautotroph, *Appl. Environ. Microbiol.*, 81, 5927-5937.

Bethke, C.M., R.A. Sanford, M.F. Kirk, Q. Jin, and T.M. Flynn (2011), The Thermodynamic Ladder in Geomicrobiology, *Am. J. Sci.,* 311, 183-210.

Bird, L.J., V. Bonnefoy, and D.K. Newman (2011), Biogenergetic challenges of microbial iron metabolisms, *Trends Microbiol.*, 19, 330-340.

Boyd, E.S., T.L. Hamilton, J.R. Havig, M.L. Skidmore, and E.L. Shock (2014), Chemolithotrophic primary production in a subglacial ecosystem, *Appl. Environ. Microb.,* 80, 6146-6153.

Bryce, R.M., and K.B. Sprague (2012), Revisiting detrended fluctuation analysis, *Sci. Rep.,* 2, 1-6.

Chan, C.S., S.C. Fakra, D. Emerson, E.J. Fleming, and K.J Edwards (2011), Lithotrophic iron-oxidizing bacteria produce organic stalks to control mineral growth: implications for biosignature formation, *ISME J.*, 5, 717-727.

Coker, A.K. (2001), *Modeling of chemical kinetics and reactor design*, Gulf Professional Publishing, USA.

Converse, B.J., J.P. McKinley, C.T. Resch, and E.E. Roden (2015), Microbial colonization across a subsurface redox transition zone, *Front. Microbiol.*, 6, 00858.

Delignieres, D., S. Ramadani, L. Lemoine, K. Torre, M. Fortes, and G. Ninot (2006), Fractal analysis for short time series: a reassessment of classical methods, *J. Math. Psy.*, 50, 525-544.

Druschel, G.K., D. Emerson, R. Sutka, P. Suchecki, and G.W. Luther (2008), Low-oxygen and chemical kinetic constraints on the geochemical niche of neutrophilic iron(II) oxidizing organisms. *Geochim. Cosmochim. Ac.,* 72, 3358-3370.

Eliazar, I.I., and M.F. Shlesinger (2013), Fractional motions, *Phys. Rep.*, 527, 101-129.

Emerson, D. (2012), Biogeochemistry and microbiology of microaerobic Fe(II) oxidation, *Biochem. Soc. Trans.*, 40, 1211-1216. doi: 10.1042/BST20120154.

Ferris, F.G. (2005), Biogeochemical properties of bacteriogenic iron oxides. *Geomicrobiol. J.*, 22, 79–85.

Ferris, F.G., R.E. James, and K. Pedersen (2015), Fragmentation of bacteriogenic iron oxides in response to hydrodynamic shear stress, *Geomicrobiol. J.*, 32, 564-569.

Ferris, F.G., A.M.L. Enright, D. Fortin, and I.D. Clark. In press. Rates of Fe(II)-oxidation and Solubility of Bacteriogenic Iron Oxides. *Geomicrobiol. J.*

Gabrielli, C., F. Huet, and H. Keddam (1993), Fluctuations in electrochemical systems. I. General theory on diffusion limited electrochemical reactions, *J. Chem. Phys.*, 99, 7232-7239.

Gault, A.G., S. Langley, A. Ibrahim, R. Renaud, Y. Takahashi, C. Boothman, J.R. Lloyd, I.D. Clark, F.G. Ferris, and D. Fortin (2012), Seasonal changes in mineralogy, geochemistry and microbial community of bacteriogenic iron oxides (BIOS) deposited in a circumneutral wetland, *Geomicrobiol. J.*, 29, 161-172.

Grigolini, P., L. Palatella, and G. Raffaelli (2001), Asymmetric anomalous diffusion: an efficient way to detect memory in time series, *Fractals*, 9, 439-449.

Hardstone, R., S.-S. Poil, G. Schiavone, R. Jansen, V.V. Nikulin, H.D. Mansvelder, and K. Linkenkaer-Hansen (2012), Detrended fluctuation analysis: a scale-free view on neuronal fluctuations. *Front. Physiol.*, 3, 450.

Hassibi, A., R. Navid, R.W. Sutton, and T.H. Lee (2004), Comprehensive study of noise processes in electrode electrolyte interfaces, *J. Appl. Phys.*, 96, 1074-1082.

Hofling, F., and T. Franosch (2013), Anomaolous transport in the crowded world of biological cells, *Rep. Prog. Phys.*, 76, 046602.

James, R.E., and F.G. Ferris (2004), Evidence for microbial-mediated iron oxidation at a neutrophilic groundwater spring, *Chem. Geol.*, 212, 301-311.

Jeon, J.-H., A.V. Chechkin, and R. Metzler (2014), Scaled Brownian motion: a paradoxical process with a time dependent diffusivity for the description of anomalous diffusion, *Phys. Chem. Chem. Phys.*, 16, 15811.

Kennedy, C.B., S.D. Scott, and F.G. Ferris (2003), Characterization of bacteriogenic iron oxide deposits from axial volcano, Juan de Fuca Ridge, Northeast Pacific Ocean, *Geomicrobiol. J.*, 20, 199-214.

Kennedy, C.B., S.D. Scott, and F.G. Ferris (2004), Hydrothermal stabilization of 2-line ferrihydrite by bacteria, *Chem. Geol.*, 212, 269-277.

MacDonald, D.J., A.J. Findlay, S.A. McAllister, J.M. Barnett, P. Hredzak-Showalter, S.T. Krepski, S.G. Cone, J. Scott, S.K. Bennett, C.S. Chan, D. Emerson, and G.W. Luther (2014), Using *in situ* voltammetry as a tool to identify and characterize habitats of iron-oxidizing bacteria: from fresh water wetlands to hydrothermal vent sites, *Environ. Sci. Process Impacts.* 16, 2117.

Melton, E.D., E.D. Swanner, S. Behrens, C. Schmidt, and A. Kappler (2014), The interplay of microbially mediated and abiotic reactions in the biogeochemical Fe cycle, *Nat. Rev. Microbiol.,* 12, 797-808.

Metzler, R. and J. Klafter (2000), The random walker's guide to anomalous diffusion: a fractional dynamics approach. *Phys. Rep.*, 339, 1-77.

Nikolausz, M., U. Kappelmeyer, A. Szekely, A. Rusznyak, K. Marialigeti, and M. Kastner (2008), Diurnal redox fluctuation and microbial activity in the rhizosphere of wetland plants, *Eur. J. Soil Biol.*, 44, 324-333.

Parsons, C.T., R.M. Couture, E.O. Omoregie, F. Bardelli, J.M. Greneche, G. Roman-Ross, and L. Charlet (2013), The impact of oscillating redox conditions: Arsenic immobilization in contaminated calcareous floodplain soils, *Environ. Pollut.*, 178, 254-263.

Peng, C.-K., S.V. Buldyrev, S. Havlin, M. Simons, H.E. Stanley, and A.L. Goldberger (1994), Mosaic organization of DNA nucleotides, *Phys. Rev. E*, 49, 1685-1689.

Petroff, F.P., T.D. Wu, B. Liang, J. Mui, J.L. Guerquin-Kern, H. Vali, D.H., Rothman, and T. Bosak (2011), Reaction-diffusion model of nutrient uptake in a biofilm: Theory and experiment. *J. Theor. Biol.*, 289, 90-95.

Rentz, J.A., C. Kraiya, G.W. Luther III., and D. Emerson (2007), Control of Ferrous Iron Oxidation within Circumneutral Microbial Iron Mats by Cellular Activity and Autocatalysis, *Environ. Sci. Technol.*, 41, 6084-6089.

Scafetta, N., and P. Grigolini (2002), Scaling detection in time series: diffusion entropy analysis, *Phys. Rev. E*, 66, 036130.

Shao, Y.H., G.F. Gu, S.Z.Q. Jiang, W.X. Zhou, and D. Sornette (2012), Comparing the performance of FA, DFA and DMA using different synthetic long-range correlated time series. *Sci. Rep.,* 2, 835. doi:10.1038/srep00835.

Stewart, P.S. (2003), Diffusion in biofilms. *J. Bacteriol.*, 185, 1485-1491.

Stumm, J., and J.J. Morgan (1996), *Aquatic chemistry: chemical equilibria and rates in natural waters*, 3rd, ed.; Wiley Interscience: U.S.A.

Suzuki, T., H. Hashimoto, N. Matsumoto, M. Furutani, H. Kunoh, and J. Takada (2011). Nanometer-scale visualization and structural analysis of the inorganic/organic hybrid structure of *Gallionella ferruginea* twisted stalks, *Appl. Environ. Microbiol.*, 77, 2877-2881.

Taillefert, M., G.W. Luther, and D.B. Nuzzio (2000), The application of electrochemical tools for *in situ* measurements in aquatic systems. *Electroanal.*, 12, 401-412.

Tolli, J. and G.M. King (2005), Diversity and structure of chemolithotrophic communities in pine forest and agroecosystem soils, *Appl. Environ. Microb.*, 71, 8411-8418.

Toner, B.M., C.M. Santelli, M.A. Marcus, R. Wirth, C.S. Chan, T. McCollom, W. Bach, and K.J. Edwards (2009), Biogenic iron oxyhydroxide formation at mid-ocean ridge hydrothermal vents: Juan de Fuca ridge, *Geochim. Cosmochim. Ac.*, 73, 388-403.

van Bochove, E., S. Beauchemin, and G. Theriault (2002), Continuous Multiple Measurement of Soil Redox Potential Using Platinum Microelectrodes, *Soil Sci. Soc. Am. J.*, 66, 1813-1820.

Vollrath, S., T. Behrends, and P. Van Cappellen (2012), Oxygen Dependency of Neutrophilic Fe(II) Oxidation by Leptothrix Differs from Abiotic Reaction, *Geomicrobiol. J.*, 29, 550-560.

Vollrath, S., T. Behrends, C.B. Koch, and P. Van Cappellen (2013), Effects of temperature on rates and mineral products of microbial Fe(II) oxidation by Leptothrix cholodnii at microaerobic conditions, *Geochim. Cosmochim. Ac.*, 108, 107-124.

Weber, K.A., L.A. Achenbach, and J.A. Coates (2006), Microorganisms pumping iron: anaerobic microbial iron oxidation and reduction, *Nat. Rev. Microbiol.*, 4, 752–764.

Table 1. Mean concentrations and standard errors for measurements of total Fe, Fe(II), and Fe(III) over a 24 hour monitoring period in the Äspö flow through cell, 297 m underground at experimental site 2200A.

Source	Concentration μM		
	Total Fe	Fe(II)	Fe(III)
Inlet	22.1 ± 0.3	21.0 ± 0.5	1.2 ± 0.8
Outlet	9.8 ± 1.6	8.5 ± 0.7	1.3 ± 0.9
Change	-12. 3 ± 1.9	-12.5 ± 1.3	0.1 ± 1.7

Table 2. The time invariant scaling exponents determined from detrended fluctuation analysis of observed and randomly shuffled redox potential time series measurements at the inlet and in the BIOS mat of the Äspö flow through cell, 297 m underground at experimental site 2200A. The observed inlet and BIOS α values are significantly different at $p < 0.01$ in one-sided t-tests.

Location in Flow Cell	Time Invariant Scaling Exponent (α value ± SE)	
	Measured	Shuffled
Inlet	1.67 ± 0.06	0.50 ± 0.01
BIOS	1.89 ± 0.03	0.51 ± 0.01

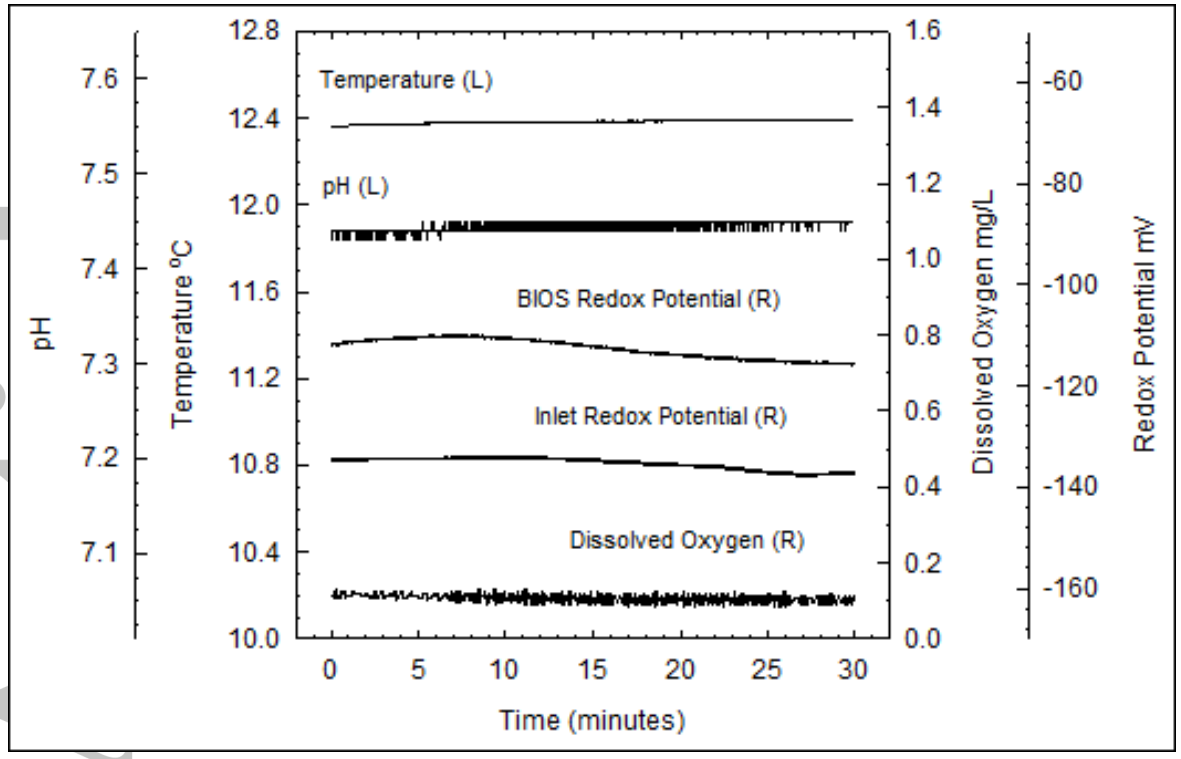

Figure 1. Temperature, pH, BIOS redox potential, inlet redox potential, and dissolved O_2 profiles over 30 minutes of data logging at one second intervals in the Äspö flow through cell, 297 m underground at experimental site 2200A.

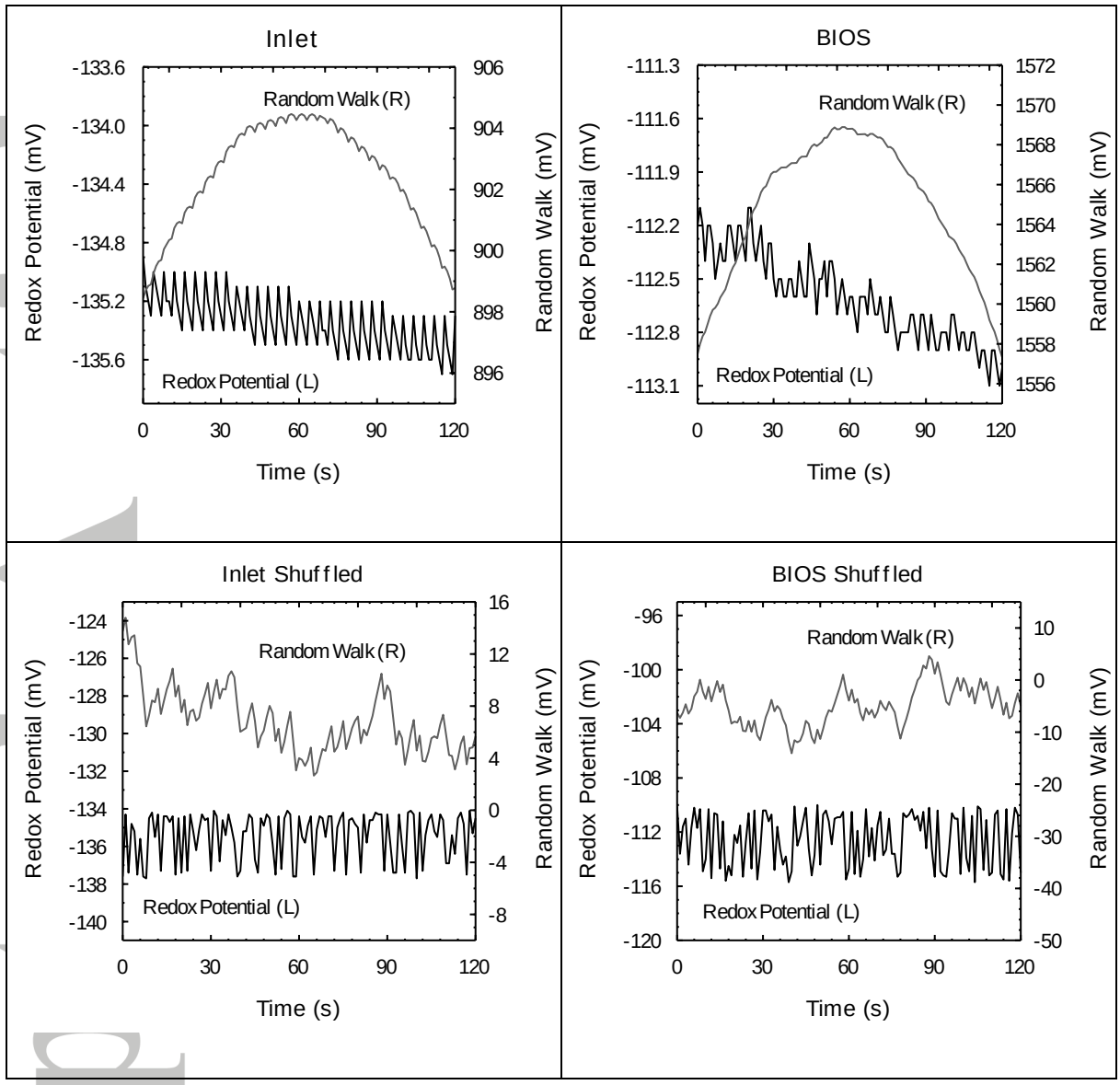

Figure 2. The observed (bottom, left axis) and random walk (top, right axis) redox potential across an interval of 120 seconds for the inlet, BIOS, and randomly shuffled time series measurements in the Äspö flow through cell, 297 m underground at experimental site 2200A.

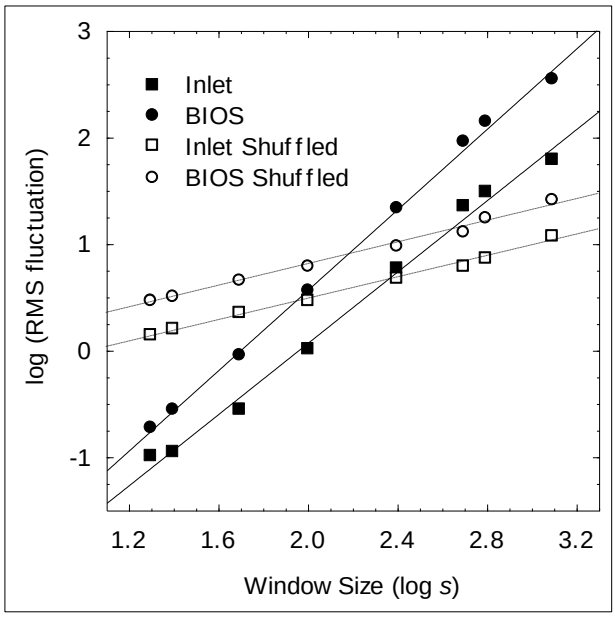

Figure 3: Log-log plot of root mean square fluctuations (mV) for inlet, BIOS, and randomly shuffled redox potential time series as a function of time interval window size *s* (seconds) in detrended fluctuation analysis.